JOURNAL OF CLINICAL MICROBIOLOGY, May 2007, p. 1426–1432 Vol. 45, No. 5
0095-1137/07/$08.00+0 doi:10.1128/JCM.01515-06

Simultaneous Quantification of Epstein-Barr Virus, Cytomegalovirus, and Human Herpesvirus 6 DNA in Samples from Transplant Recipients by Multiplex Real-Time PCR Assay[▽]

Kaoru Wada,[1] Naomi Kubota,[1] Yoshinori Ito,[2] Hiroshi Yagasaki,[2] Koji Kato,[3] Tetsushi Yoshikawa,[4] Yasuyuki Ono,[5] Hisami Ando,[5] Yasuhiro Fujimoto,[6] Tetsuya Kiuchi,[6] Seiji Kojima,[2] Yukihiro Nishiyama,[1] and Hiroshi Kimura[1]*

Departments of Virology,[1] Pediatrics,[2] Pediatric Surgery,[5] and Transplant Surgery,[6] Nagoya University Graduate School of Medicine, Nagoya, Japan; Department of Pediatrics, Japanese Red Cross Nagoya First Hospital, Nagoya, Japan[3]; and Department of Pediatrics, Fujita Health University School of Medicine, Toyoake, Japan[4]

Received 22 July 2006/Returned for modification 31 October 2006/Accepted 12 March 2007

We developed a multiplex real-time PCR assay using 6-carboxyfluorescein, 6-carboxy-4′,5′-dichloro-2′,7′-dimethoxyfluorescein, and carbocyanine 5-labeled probes to simultaneously quantify Epstein-Barr virus (EBV), cytomegalovirus (CMV), and human herpesvirus 6 (HHV-6) DNA. When previously tested and stored DNA samples were examined, results of the multiplex real-time PCR assay were as sensitive and specific as those of a single real-time PCR assay. The multiplex assay was used to quantify the EBV, CMV, and HHV-6 DNA in 46 transplant recipients. A total of 303 whole-blood and plasma specimens were collected and analyzed. According to the results of the multiplex assay, the detection rates for viral DNA in whole blood and plasma were 23.8% and 5.9% for EBV, 11.2% and 5.3% for CMV, and 12.5% and 2.0% for HHV-6, respectively. All forms of viral DNA were detected more frequently in whole blood than in plasma. During the symptomatic period, EBV DNA was detected in all whole-blood specimens but not in all plasma specimens. Furthermore, the EBV DNA load in whole blood was higher during the symptomatic period than during the asymptomatic period, whereas the EBV DNA load in plasma was similar for both periods. These results demonstrate that whole blood is more suitable for the quantification of EBV DNA in transplant patients. However, a cutoff value with clinical relevance still needs to be determined.

Herpesviruses are ubiquitous in the human population and often become reactivated in latently infected immunocompromised patients (4, 22). Herpesvirus reactivation frequently occurs after hematopoietic stem cell or solid-organ transplantation and occasionally results in symptomatic diseases (2, 4, 28). Among human herpesviruses, Epstein-Barr virus (EBV), cytomegalovirus (CMV), and human herpesvirus 6 (HHV-6) may cause life-threatening complications, such as lymphoproliferative disorders (3, 13, 27), interstitial pneumonia (7, 15), and encephalitis (2, 12, 23, 25). Therefore, to ensure the success of transplantation, it is essential to monitor for these viruses and diagnose any virus-related diseases as early as possible.

With the advent of real-time PCR technology, quantitative PCR assays are becoming widespread methodologies for diagnostic purposes (9, 11). We initially developed quantitative real-time PCR systems to detect EBV (5), CMV (18), and HHV-6 DNA (19). However, because each system was able to detect only one form of viral DNA, simultaneous virus monitoring was cost, time, and labor intensive. It was recently shown that quantification of more than one target per well is possible with the use of different fluorochromes (1, 14, 21, 24). One aim of the present study was to establish a system for the simultaneous quantification of EBV, CMV, and HHV-6 DNA by using a multiplex real-time PCR assay. Another goal was to identify specimens that would optimize virus monitoring. While peripheral blood cells, whole blood, and plasma are commonly used in quantitative real-time PCR, whole blood and plasma are more convenient to use and are suitable for clinical analysis. Since whole blood contains peripheral blood cells, we considered that whole blood could be used instead of peripheral blood cells. In the present study, we developed a multiplex real-time PCR assay to quantify EBV, CMV, and HHV-6 DNA. In addition, we sought to determine whether whole blood or plasma was more suitable for simultaneous virus monitoring in samples from transplant recipients.

MATERIALS AND METHODS

Patients and clinical specimens. In total, 27 hematopoietic stem cell transplantation recipients (16 men, 11 women) and 19 liver transplantation recipients (9 men, 10 women) were enrolled in the study. Beginning 1 week after transplantation, EDTA blood samples were prospectively obtained from subjects weekly until they were discharged. From 46 patients, 1 to 13 samples per patient (total 303, mean 6.6) were collected from 1 to 15 weeks after transplantation (mean 7.8 weeks). From some patients, only a few samples could be obtained because of their early death or follow-up loss. Informed consent was obtained from all patients or guardians. The institutional review board of Nagoya University Hospital approved the use of specimens included in this study.

Among the hematopoietic stem cell transplantation recipients, 10 had acute leukemia, 6 had severe aplastic anemia, 4 had solid tumors, 2 had chronic leukemia, and 5 had other diseases. The patients underwent transplantation between November 2003 and October 2005 at Nagoya University Hospital or at Japanese Red Cross Nagoya First Hospital. The median age of the patients was 8.0 years (range, 1 to 22 years). Eight of 27 patients received antithymocyte globulin, which is known to be a risk factor for EBV-related lymphoproliferative disorders (3, 13).

* Corresponding author. Mailing address: Department of Virology, Nagoya University Graduate School of Medicine, 65 Tsuruma-cho, Showa-ku, Nagoya 466-8550, Japan. Phone: 81-52-744-2207. Fax: 81-52-744-2452. E-mail: hkimura@med.nagoya-u.ac.jp.

▽ Published ahead of print on 21 March 2007.

TABLE 1. Sequences of primers and probes used in the real-time PCR assay

Target gene (GenBank accession no.)	Primer or probe	Sequence (5′→3′)[a]	Genome coordinate
EBV BALF5 (AJ507799)	Forward primer	CGGAAGCCCTCTGGACTTC	156007–156025
	Reverse primer	CCCTGTTTATCCGATGGAATG	155936–55956
	Probe	FAM-TGTACACGCACGAGAAATGCGCC-BHQ1a	155959–155981
CMV IE (NC001347)	Forward primer	GACTAGTGTGATGCTGGCCAAG	172435–172456
	Reverse primer	GCTACAATAGCCTCTTCCTCATCTG	172256–172270
	Probe	JOE-AGCCTGAGGTTATCAGTGTAATGAAGCGCC-BHQ1a	172389–172418
HHV-6 U31 (AF157706)	Forward primer	TTTGCAGTCATCACGATCGG	46661–46680
	Reverse primer	AGAGCGACAAATTGGAGGTTTC	46862–46883
	Probe	Cy5-AGCCACAGCAGCCATCTACATCTGTCAA-BHQ3a	46753–46780

[a] FAM, 6-carboxyfluorescein; JOE, 6-carboxy-4′,5′-dichloro-2′,7′-dimethoxyfluorescein; Cy5, carbocyanine 5.

The liver transplantation recipients received their organs from living donors at Nagoya University Hospital between February 2004 and December 2005. Of 19 patients, 8 had hepatic cirrhosis (hepatitis B virus, 3; hepatitis C virus, 2; other viruses, 3), 3 had biliary atresia, and 8 had other diseases. The median age of the patients was 48.0 years (range, 6 months to 62 years).

Symptomatic EBV infections were diagnosed from clinical findings (fever, enlarged lymph nodes, and hematochezia) and serological examinations. A lymph node biopsy provided histological confirmation that one patient with symptomatic EBV infection had posttransplant lymphoproliferative disorder. CMV hepatitis was diagnosed from the clinical findings and serological examination and confirmed by liver biopsy.

A total of 303 consecutive blood specimens were obtained from transplant recipients and divided into whole-blood or plasma samples, and the 303 paired samples were tested with the multiplex real-time PCR assay. Viral DNA was extracted from 200 μl of whole blood or 200 μl of plasma, using QIAamp DNA blood kits (QIAGEN, Hilden, Germany) and eluted in 100 μl of water.

Specificity and sensitivity studies were performed with 111 DNA samples that had been obtained from other transplantation recipients. These DNA samples had been extracted from either whole-blood or plasma samples and used to monitor viruses by either qualitative PCR or real-time PCR, and stored at −30°C.

The specificity was also confirmed with viral DNA from standard strains (KOS for herpes simplex virus type 1, 186 for herpes simplex virus type 2, Kawaguchi strain for varicella-zoster virus, B95-8 for EBV, AD169 for CMV, Sato strain for HHV-7, and a clinical isolate from a patient with exanthem subitum for HHV-6). Viral DNA was extracted from the supernatant of each virus culture and was used for the cross-reactivity study.

EDTA blood was taken from a patient who was seronegative for EBV, CMV, and HHV-6, and plasma was separated. A DNA extraction solution from either the whole blood or the plasma fraction was used for reconstruction studies.

Primers and probes. The sequences of the primers and probes used for the multiplex real-time PCR assay are listed in Table 1. The primer and probe sets for the viruses have been described previously (5, 18, 19). Each probe was labeled with different fluorochromes, as follows: the EBV probe was labeled with 6-carboxyfluorescein and quenched with Black-Hole-Quencher 1a (BHQ1a); the CMV probe was labeled with 6-carboxy-4′,5′-dichloro-2′,7′-dimethoxyfluorescein and quenched with BHQ1a; the HHV-6 probe was labeled with carbocyanine 5 and quenched with BHQ3a. All primers (Fasmac, Kanagawa, Japan) and probes (Operon Biotechnologies, Huntsville, AL) were synthesized commercially.

Quantification of viral DNA by multiplex real-time PCR. Multiplex and independent real-time PCR were performed with a QuantiTect multiplex PCR kit (QIAGEN). The multiplex real-time PCR assay was performed in a total reaction mixture (25 μl) containing 5 μl of DNA extracts, 12.5 μl of 2× QuantiTect multiplex PCR master mix, each forward and reverse primer, and each probe. To determine the optimal concentrations of the primers and probes, we evaluated various concentrations of primer and probe sets using the multiplex real-time PCR assay. The optimal concentration of forward primer was 200 nM for EBV and 100 nM for CMV and HHV-6. The optimal concentration of reverse primer was 200 nM for EBV, 100 nM for CMV, and 200 nM for HHV-6. The optimal concentration of each probe was 100 nM. The independent real-time PCR was performed in the same way as the multiplex real-time PCR assay except that only one primer/probe set was included. Amplification and real-time fluorescence detection were performed with a model Mx3000P real-time PCR system (Stratagene, La Jolla, CA) using the following protocol: an initial denaturation and polymerase activation step for 15 min at 95°C, followed by 50 cycles of denaturation at 95°C for 15 s and 60°C for 1 min. Real-time fluorescence measurements were taken, and a threshold cycle value for each sample was calculated by determining the point at which the fluorescence exceeded a threshold limit. Each real-time PCR assay contained the dilution series of a standard for the calibration curve, and all samples and the standard were run in duplicate. The standards were plasmid controls that contained the PCR products amplified by each primer set, as described previously (5, 18, 19). For the multiplex real-time PCR, each plasmid control was mixed, diluted, and used to make calibration curves. The number of viral DNA copies was calculated from the standard curves and expressed as copies per 1 ml of whole blood or plasma.

CMV antigenemia assay. The CMV antigenemia assay was performed as previously described (18). The approximate antigenemia threshold was 1 positive cell per 5×10^4 leukocytes, as determined by guidelines from the Japanese Society for Hematopoietic Cell Transplantation. When the antigenemia assay was positive, patients were administered ganciclovir preemptively.

Statistical analysis. StatView J 4.02 (Abacus Concepts Inc., Berkeley, CA) was used to perform the data analysis. A regression analysis compared the multiplex assay with the single assay. Fisher's exact test was used to compare the viral DNA detection rates, and Student's t test was used to compare the mean viral DNA $\log_{10}$ copy numbers. To determine the minimum detection level of each assay, 35 replicates each of one, two, and five copies of the plasmid standard were quantified. The 95% confidence interval (CI) was calculated from the t distribution using the following formula: 95% CI = the mean of the estimated copy number $\pm$ $t \times$ standard error, where t was estimated to be 2.042 from the Student's t table.

RESULTS

Specificity and sensitivity of the multiplex quantification using an Mx3000P real-time PCR system. Serial dilutions of mixed viral standard plasmids were tested with the multiplex assay, and three standard curves were constructed from the cycle of threshold values. The assay was able to detect each viral DNA form over a linear span between 5 and 5×10^6 copies per reaction mixture without interference (Fig. 1). The standard curves generated from the multiplex real-time PCR were almost equal to those generated from the single assay. Because amplification efficiency may be influenced by the background DNA of the clinical specimen, we evaluated the performance of the multiplex assay using standard plasmids diluted in water or in water containing EBV-, CMV-, and HHV-6-negative human genomic DNA. The standard curves generated from the standard plasmids in background DNA were almost equal to those generated from the standard plasmids in water, indicating that amplification efficiency was not influenced by the background DNA (data not shown). We also performed reconstruction studies to confirm the absence of the

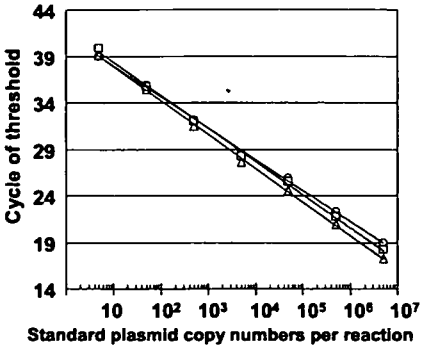

FIG. 1. Standard curves generated by multiplex real-time PCR. Serial dilutions of each viral standard ranging from 5 to 5 × 10^6 copies per reaction were used to generate the standard curves. The cycle of threshold values that corresponded to the PCR cycle number was plotted against the copy number of each viral standard. Circles, EBV DNA standard plasmid; triangles, CMV DNA standard plasmid; squares, HHV-6 standard plasmid.

inhibitor from whole-blood or plasma samples. DNA-extraction solution from either whole blood or plasma was added to serially diluted plasmid controls. The DNA solutions from both whole blood and plasma did not inhibit the amplification efficiency, indicating the absence of inhibitors in these samples. To confirm the specificity of the multiplex assay, viral DNA from standard strains was tested. None of the primer/probe sets reacted with the other viral DNA, indicating that no cross-reactivity occurred. Furthermore, the quantitative linearity, which was made using a standard plasmid, was not influenced by the presence of two other kinds of viral DNA.

The minimum detection level established with this multiplex assay was 2 copies per reaction for EBV (95% CI, 1.16 to 3.89), 2 copies for CMV (95% CI, 1.01 to 2.95), and 2 copies for HHV-6 (95% CI, 0.49 to 2.64). By contrast, the minimum detection level with the single assay was 2 copies for EBV (95% CI, 1.39 to 3.96), 2 copies for CMV (95% CI, 1.01 to 2.71), and 5 copies for HHV-6 (95% CI, 4.35 to 7.58). The multiplex assay had an overall dynamic range of 200 to 5 × 10^8 copies/ml of specimen.

DNA samples (111), which had been tested and stored previously, were evaluated with the multiplex and the single assays. Compared to the results of the single assay, the sensitivity and specificity values of the multiplex assay were 96.0 and 100% for EBV, 94.7 and 95.7% for CMV, and 89.2 and 94.6% for HHV-6, respectively (Table 2). Some discordant results, however, were obtained between the multiplex and single assays. The viral loads of all of these discordant samples were low and around the detection limits. The viral DNA copy numbers were compared using all samples determined to be positive according to both assays. Strong correlations were detected between the viral DNA copy numbers determined by the multiplex assays and those by single assays (Fig. 2). The slopes of the correlation curves ranged from 0.957 to 1.133, indicating that no significant shifts occurred in the actual quantitative values, using the multiplex assay.

TABLE 2. Comparison of multiplex PCR assay and single PCR assay of previously tested DNA samples

Multiplex PCR assay	Single PCR assay (copies/ml)		Sensitivity (%)	Specificity (%)
	Positive	Negative		
EBV				
No. positive	24	0	96.0	100
No. negative	1	86		
CMV				
No. positive	18	4	94.7	95.7
No. negative	1	88		
HHV-6				
No. positive	33	4	89.2	94.6
No. negative	4	70		

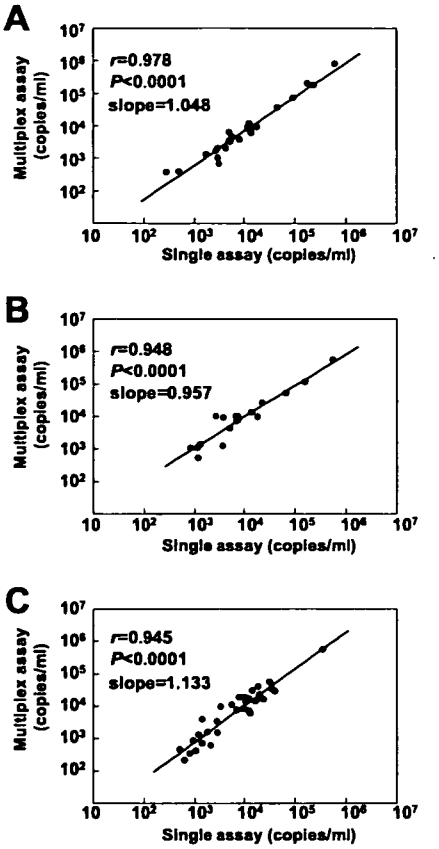

FIG. 2. Correlation of each viral DNA load determined by the multiplex and single real-time PCR assays. (A) Correlation of EBV DNA copy number (n = 24). (B) Correlation of CMV DNA copy number (n = 18). (C) Correlation of HHV-6 DNA copy number (n = 33).

Detection of EBV, CMV, and HHV-6 DNA in whole-blood and plasma specimens from transplant recipients. Using the multiplex real-time PCR assay, we serially measured the EBV, CMV, and HHV-6 DNA levels in whole-blood and plasma specimens from 46 transplant recipients. In total, 303 paired samples (6.6 paired samples per patient) were tested. Positives were defined as any positive samples for a given patient. Because we had different numbers of samples from each patient, it was possible that the variety of sample numbers per patient would introduce some bias in the results. Using the whole-blood specimens, at least one form of viral DNA was detected in 36 of 46 recipients (78.3%), plural viral DNA forms were

TABLE 3. Detection of EBV, CMV, and HHV-6 DNA in whole blood and plasma using multiplex real-time PCR assay

Detected viral DNA	No. of samples detected from: Whole blood (n = 303)		Plasma (n = 303)		P value[a]
	n	%	n	%	
EBV or CMV or HHV-6	112	37.0	37	12.2	<0.0001
EBV	72	23.8	18	5.9	<0.0001
CMV	34	11.2	16	5.3	0.0114
HHV-6	38	12.5	6	2.0	<0.0001
EBV only	48	15.8	15	5.0	
CMV only	16	5.3	13	4.3	
HHV-6 only	19	6.3	6	2.0	
EBV and CMV	10	3.3	3	1.0	
CMV and HHV-6	5	1.7	0	0	
EBV and HHV-6	11	3.6	0	0	
EBV, CMV, and HHV-6	3	1.0	0	0	
Below detection limits in all viruses	191	63.0	266	87.8	

[a] Fisher's exact test.

detected in 13 recipients (28.3%), and all three viral DNA forms were detected in 3 recipients (6.5%). Using the plasma specimens, at least one viral DNA form was detected in 18 of 46 recipients (39.1%), and plural viral DNA forms were detected in 5 recipients (10.9%).

Four patients who underwent hematopoietic stem cell transplantation developed symptomatic EBV infections and were preconditioned with antithymocyte globulin. The patients had prolonged fever, lymphadenopathy, diarrhea, or hematochezia, which could not be explained by other causes. One patient who underwent liver transplantation developed CMV hepatitis despite preemptive ganciclovir therapy. None of the patients developed HHV-6-related diseases. Each form of viral DNA was detected in both the whole-blood and plasma specimens of these five symptomatic patients, and the peaks of the viral DNA loads were concordant with the symptoms observed.

Of the 303 whole-blood samples tested, 112 were positive for at least one viral DNA form, and 29 were positive for plural viral DNA forms. Conversely, 37 of 303 plasma samples were positive for at least one viral DNA form, and only 3 samples were positive for plural viral DNA forms (Table 3). The detection rates of viral DNA in whole blood and plasma were 23.8% and 5.9% for EBV, 11.2% and 5.3% for CMV, and 12.5% and 2.0% for HHV-6, respectively. The three viral DNA forms of interest were detected more frequently in whole blood than in plasma. EBV DNA loads ranged from 220 to 8.6×10^6 copies/ml in whole blood and from 250 to 7.5×10^4 copies/ml in plasma. CMV DNA loads ranged from 220 to 3.8×10^5 copies/ml in whole blood and from 200 to 8.5×10^4 copies/ml in plasma. HHV-6 DNA loads ranged from 240 to 1.3×10^5 copies/ml in whole blood and from 290 to 1.1×10^4 copies/ml in plasma. The viral DNA copy numbers were compared using samples determined to be positive in both whole blood and plasma (Fig. 3). Weak correlations were seen between the viral loads in whole blood and those in plasma.

Comparison of EBV DNA loads between whole blood and plasma. We divided the 303 samples into two groups based on EBV infection-related symptoms, symptomatic and asymptomatic. In the symptomatic group, EBV DNA was detected in all nine whole-blood samples with high viral loads but not in two plasma samples (Fig. 4). Among the whole-blood samples, the viral loads of the symptomatic group were significantly higher than those of the asymptomatic group. However, among the plasma samples, the viral loads were similar between the two groups (Fig. 4).

Comparison of antigenemia and multiplex real-time PCR assays. The antigenemia assay was applied to 235 of 303 blood specimens that had been evaluated with the multiplex assay. CMV antigen was detected in 13 of 235 blood samples (5.5%). With the multiplex assay, CMV DNA was detected in 32 of 235 whole-blood specimens (13.6%; $P = 0.002$ versus antigenemia) and 14 of 235 plasma specimens (6.0%; $P = 0.5$ versus antigenemia). When the antigenemia assay was defined as the standard, the specificity of CMV DNA detection was higher for the plasma specimens than for the whole-blood specimens (Table 4). On the other hand, the sensitivity seemed to be higher for the whole-blood specimens, although statistical significance was not achieved, probably due to the small sample size.

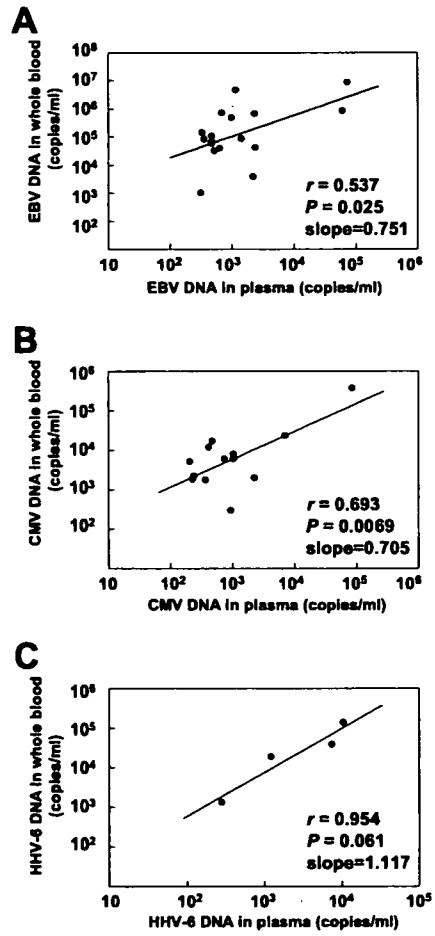

FIG. 3. Correlation of each viral DNA load between whole blood and plasma. (A) Correlation of EBV DNA copy number (n = 17). (B) Correlation of CMV DNA copy number (n = 13). (C) Correlation of HHV-6 DNA copy number (n = 4). The viral DNA copy numbers were compared using samples determined to be positive in both whole blood and plasma.

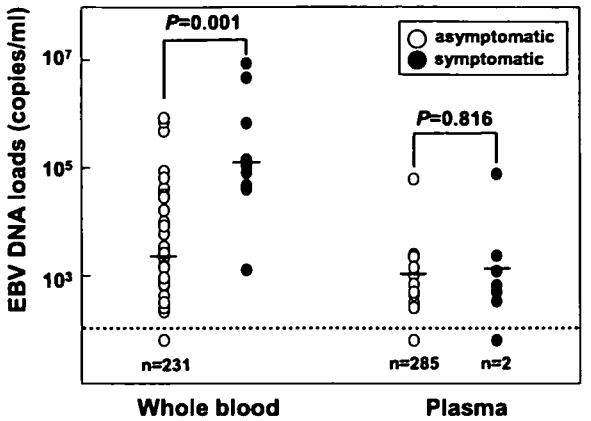

FIG. 4. Comparison of EBV DNA loads between whole-blood and plasma specimens. The dotted line indicates the detection limit in this assay. Bars show the mean copy numbers of EBV DNA. *n*, number of undetectable samples.

The 235 specimens were classified into four categories by the antigenemia values (negative, 0; low, 1 to 10; intermediate, 11 to 100; high, >100), and CMV DNA loads were compared (Table 5). Although the sample numbers for each group were small, it appeared that CMV DNA loads increased in proportion to increases in the antigenemia values. Correlations between antigenemia values and CMV DNA loads were then analyzed using the positive samples. Antigenemia values were significantly correlated with CMV DNA loads, both in whole blood ($n = 12$; $r = 0.776$; $P = 0.002$) and in plasma ($n = 9$; $r = 0.861$; $P = 0.002$).

Monitoring of EBV, CMV, and HHV-6 DNA loads in a transplant recipient. Figure 5 shows changes in the viral DNA loads in a representative case. The patient was a 4-year-old girl with severe aplastic anemia who underwent bone marrow transplantation. Two weeks after transplantation, CMV DNA was detected in her whole-blood and plasma samples (Fig. 5). Shortly after the detection of CMV DNA, the patient's blood tested positive for the CMV antigen. Although the patient had no symptoms associated with CMV infection, ganciclovir was administered preemptively. Her CMV DNA load decreased in accordance with the ganciclovir therapy. During treatment, a high level of EBV DNA was detected in her blood. In the fifth week after transplantation, she developed a fever and hematochezia. Since EBV DNA had been detected at a high level in her whole blood and plasma and other pathogens and causes that may have explained her symptoms were excluded, an EBV-related lymphoproliferative disorder was suspected. Immunosuppression was tapered, but that was not effective. Therefore, the monoclonal anti-CD20 antibody rituximab was administered. Immediately after rituximab administration, her EBV DNA load decreased in conjunction with her clinical symptoms. During the period of viral monitoring, HHV-6 DNA was undetectable in her whole blood and plasma.

DISCUSSION

Real-time PCR is a powerful tool for quantifying gene targets using fluorogenic probes and real-time laser scanning. Although multiplex real-time PCR is theoretically possible using probes with spectrally different fluorophores, the overlap of fluorophores prevents accurate quantification and limits amplification to two genes per tube (21). Only two targets could be quantified reliably in a single tube. However, recent advances in the development of real-time PCR platforms and master mix have made it possible to quantify more than three different genes in a single tube (21).

To our knowledge, this is the first study using the multiplex real-time PCR assay in the quantification of EBV, CMV, and HHV-6 DNA. Our results showed that the multiplex assay was as sensitive and specific as the single real-time PCR assay. The viral DNA loads determined by the multiplex real-time PCR assay were consistent with those described previously using other assays (6–8, 12, 26). Monospecific PCR assays require separate amplification of each target and are therefore more cost, time, and labor intensive than multiplex assays. The multiplex real-time PCR assay offers a major advantage in the field of clinical virology as it permits simultaneous amplification of several viruses in a single reaction mixture (1, 14, 21). The multiplex real-time PCR assay is particularly useful in the management of posttransplant patients, in whom frequent viral monitoring is required. The multiplex assay facilitates cost-effective diagnosis and may contribute to a decrease in the use of antiviral agents and in viral complications and hospitalizations.

One aim of the present study was to determine whether whole blood or plasma was more suitable for simultaneous virus monitoring in transplant recipients. EBV latently infects B lymphocytes. In EBV-associated lymphoproliferative disorders, EBV-infected B lymphocytes are usually found in the blood (27). Therefore, peripheral blood mononuclear cells are the best specimens to use in quantifying the EBV DNA load in transplant patients. However, whole blood, which contains mononuclear cells and is convenient to use, has been suggested as an acceptable alternative (17, 26). CMV latently infects a variety of leukocytes but predominantly cells in the monocyte/macrophage lineage. CMV quantification can be performed with acellular fractions of the blood, such as plasma and serum (7, 20, 29); however, in transplant recipients, the quantity of viral DNA is greater in leukocytes than in plasma (6, 10). HHV-6, which is closely related to CMV, infects mainly $CD4^+$ T lymphocytes and is predominantly found in latently infected monocytes/macrophages (28). Since considerable amounts of

TABLE 4. Comparison of multiplex real-time PCR assay and antigenemia assay of 235 blood specimens

Multiplex real-time PCR	Antigenemia assay		% of sensitivity (95% CI)	% of specificity (95% CI)
	No. of positive samples	No. of negative samples		
Whole-blood specimens				
No. positive	12	20	92.3%[a]	91.0%[b]
No. negative	1	202	(77.8–100)	(97.2–94.8)
Plasma specimens				
No. positive	9	5	69.2%[a]	97.7%[b]
No. negative	4	217	(44.1–94.3)	(95.8–99.7)

[a] $P = 0.32$ by Fisher's exact test.
[b] $P = 0.003$ by Fisher's exact test.

TABLE 5. CMV DNA loads determined by multiplex real-time PCR assay in comparison with the antigenemia assay

Categories of antigenemia values (positive cells/ 5×10^4 cells)	Median antigenemia values (range)	No. of tested specimens	CMV DNA loads (copies/ml)			
			Whole blood		Plasma	
			No. of positive samples	Median (range)	No. of positive samples	Median (range)
0		222	20	1,420 (250–11,810)	5	280 (230–950)
1–10	2.0 (1–4)	10	9	5,040 (430–17,000)	6	620 (200–1,060)
11–100	17.5 (16–19)	2	2	12,450 (1,980–22,920)	2	4,740 (2,250–7,230)
>100	103	1	1	375,500	1	85,480

the HHV-6 genome persist in monocytes/macrophages, detection of HHV-6 DNA in whole blood may reflect both latent and active viral infection. Therefore, it has been suggested that the HHV-6 viral load in plasma is an effective indicator of active infection (16, 28).

In the present study, we compared whole-blood and plasma specimens in the simultaneous detection of EBV, CMV, and HHV-6 DNA. The detection rate for each viral DNA form was higher in the whole-blood specimens than in the plasma specimens. During the symptomatic periods, EBV DNA was found in all whole-blood specimens obtained but not in all plasma specimens. EBV DNA loads in whole blood were higher during the symptomatic period than during the asymptomatic period, whereas EBV DNA loads in plasma were similar during both periods. These results support the use of whole-blood specimens for multiplex real-time PCR assays in transplant patients, although we have insufficient data to conclude that whole blood is preferable for assaying CMV and HHV-6 loads. On the other hand, EBV, CMV, and HHV-6 latently infect blood corpuscles, and asymptomatic reactivation may occur in transplant patients. Therefore, it is necessary to determine a cutoff value that reflects clinical relevance. In this study, we could not determine the cutoff value because of the sample size and heterogeneity of the transplantations. Since the number of peripheral blood cells varies, especially after stem cell transplantation, this may influence the viral load in whole blood. A large prospective study to determine the clinical cutoff value for each virus and each transplantation type is currently under way.

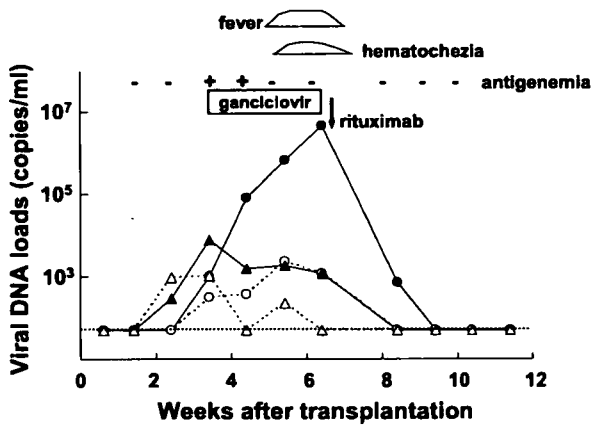

FIG. 5. Monitoring of viral DNA loads by multiplex real-time PCR in a 4-year-old girl who underwent bone marrow transplantation. Closed circles, EBV DNA copy number in whole blood; open circles, EBV DNA in plasma; closed triangles, CMV DNA in whole blood; open triangles, CMV DNA in plasma. The dotted line indicates the detection limit in this assay.

In summary, we developed a multiplex real-time PCR assay for the simultaneous detection of EBV, CMV, and HHV-6 DNA. The results of the multiplex assay were as sensitive and specific as those of the single real-time PCR assay. Compared to plasma, whole blood was more suitable for quantifying EBV DNA in transplant patients. The savings in cost, time, and labor associated with multiplex real-time PCR validate its use in the management of transplant recipients.

ACKNOWLEDGMENTS

We thank the following individuals for their contributions to this study: Yukiko Watanebe, Kenichiro Kaneko, Youhei Yamauchi (Nagoya University Graduate School of Medicine), and Hideki Muramatsu (Japanese Red Cross Nagoya First Hospital).

This study was supported by grants from the Ministry of Education, Culture, Sport, Science and Technology of Japan (17209037).

REFERENCES

1. **Adelson, M. E., M. Feola, J. Trama, R. C. Tilton, and E. Mordechai.** 2005. Simultaneous detection of herpes simplex virus 1 and 2 by real-time PCR and pyrosequencing. J. Clin. Virol. **33**:25–34.
2. **Hentrich, M., D. Oruzio, G. Jäger, M. Schlemmer, M. Schleuning, X. Schiel, W. Hiddemann, and H.-J. Kolb.** 2005. Impact of human herpesvirus-6 after haematopoietic stem cell transplantation. Br. J. Haematol. **128**:66–72.
3. **Hoshino, Y., H. Kimura, N. Tanaka, I. Tsuge, K. Kudo, K. Horibe, K. Kato, T. Matsuyama, A. Kikuta, S. Kojima, and T. Morishima.** 2001. Prospective monitoring of the Epstein-Barr virus DNA by a real-time quantitative polymerase chain reaction after allogenic stem cell transplantation. Br. J. Haematol. **115**:105–111.
4. **Jenkins, F. J., D. T. Rowe, and C. R. Rinaldo, Jr.** 2003. Herpesvirus infections in organ transplant recipients. Clin. Diagn. Lab. Immunol. **10**:1–7.
5. **Kimura, H., M. Morita, Y. Yabuta, K. Kuzushima, K. Kato, S. Kojima, T. Matsuyama, and T. Morishima.** 1999. Quantitative analysis of Epstein-Barr virus load by using a real-time PCR assay. J. Clin. Microbiol. **37**:132–136.
6. **Li, H., J. S. Dummer, W. R. Estes, S. Meng, P. F. Wright, and Y.-W. Tang.** 2003. Measurement of human cytomegalovirus loads by quantitative real-time PCR for monitoring clinical intervention in transplant recipients. J. Clin. Microbiol. **41**:187–191.
7. **Limaye, A. P., M.-L. Huang, W. Leisenring, L. Stensland, L. Corey, and M. Boeckh.** 2001. Cytomegalovirus (CMV) DNA load in plasma for the diagnosis of CMV disease before engraftment in hematopoietic stem-cell transplant recipients. J. Infect. Dis. **183**:377–382.
8. **Macé, M., C. Manichanh, P. Bonnafous, S. Précigout, D. Boutolleau, A. Gautheret-Dejean, and H. Agut.** 2003. Real-time PCR as a versatile tool for investigating the susceptibility of human herpesvirus 6 to antiviral agents. Antimicrob. Agents Chemother. **47**:3021–3024.
9. **Mackay, I. M., K. E. Arden, and A. Nitsche.** 2002. Real-time PCR in virology. Nucleic Acids Res. **30**:1292–1305.
10. **Mengelle, C., K. Sandres-Saunè, C. Pasquier, L. Rostaing, J.-M. Mansuy, M. Marty, I. Da Silva, M. Attal, P. Massip, and J. Izopet.** 2003. Automated extraction and quantification of human cytomegalovirus DNA in whole blood by real-time PCR assay. J. Clin. Microbiol. **41**:3840–3845.
11. **Niesters, H. G. M.** 2004. Molecular and diagnostic clinical virology in real time. Clin. Microbiol. Infect. **10**:5–11.

12. **Ogata, M., H. Kikuchi, T. Satou, R. Kawano, J. Ikewaki, K. Kohno, K. Kashima, E. Obtsuka, and J. Kadota.** 2006. Human herpesvirus 6 DNA in plasma after allogeneic stem cell transplantation: incidence and clinical significance. J. Infect. Dis. 193:68–79.
13. **Peres, E., S. Savasan, J. Klein, M. Abidi, R. Dansey, and E. Abella.** 2005. High fatality rate of Epstein-Barr virus-associated lymphoproliferative disorder occurring after bone marrow transplantation with rabbit anti-thymocyte globulin conditioning regimens. J. Clin. Microbiol. 43:3540–3543.
14. **Pradeau, K., L. Couty, J.-C. Szelag, P. Turlure, F. Rolle, P. Ferrat, D. Borsessoule, Y. L. Meur, F. Denis, and S. Ranger-Rogez.** 2006. Multiplex real-time PCR assay for simultaneous quantitation of human cytomegalovirus and herpesvurus-6 in polymorphonuclear and mononuclear cells of transplant recipients. J. Virol. Methods 132:77–88.
15. **Razonable, R. R., R. A. Brown, A. Humar, E. Covington, E. Alecock, C. V. Paya, and the PV16000 Study Group.** 2005. Herpesvirus infections in solid organ transplant patients at high risk of primary cytomegalovirus disease. J. Infect. Dis. 192:1331–1339.
16. **Secchiero, P., D. R. Carrigan, Y. Asano, L. Benedetti, R. W. Crowley, A. L. Komaroff, R. C. Gallo, and P. Lusso.** 1995. Detection of human herpesvirus 6 in plasma of children with primary infection and immunosuppressed patients by polymerase chain reaction. J. Infect. Dis. 171:273–280.
17. **Stevens, S. J. C., S. A. W. M. Verkuijilen, A. J. C. van den Brule, and J. M. Middeldorp.** 2002. Comparison of quantitative competitive PCR with LightCycler-based PCR for measuring Epstein-Barr virus DNA load in clinical specimens. J. Clin. Microbiol. 40:3986–3992.
18. **Tanaka, N., H. Kimura, K. Iida, Y. Saito, I. Tsuga, A. Yoshimi, T. Matsuyama, and T. Morishima.** 2000. Quantitative analysis of cytomegalovirus load using a real-time PCR assay. J. Med. Virol. 60:445–462.
19. **Tanaka, N., H. Kimura, Y. Hoshino, K. Kato, T. Yashikawa, Y. Asano, K. Horibe, S. Kojima, and T. Motishima.** 2000. Monitoring four herpesviruses in unrelated cord blood transplantation. Bone Marrow Transplant. 26:1193–1197.
20. **Tedder, R. S., U. Ayliffe, W. Preiser, N. S. Brink, P. R. Grant, K. S. Peggs, S. Mackinnon, F. Kreig-Schneider, S. Kirk, and J. A. Garson.** 2002. Development and evaluation of an internally controlled semiautomated PCR assay for quantification of cell-free cytomegalovirus. J. Med. Virol. 66:518–523.
21. **Templeton, K. E., S. A. Scheltinga, N. F. C. Beersma, A. C. M. Kroes, and E. C. J. Claas.** 2004. Rapid and sensitive method using multiplex real-time PCR for diagnosis of infections by influenza A and influenza B viruses, respiratory syncytial virus, and parainfluenza viruses 1, 2, 3, and 4. J. Clin. Microbiol. 42:1564–1569.
22. **Timbury, M. C., and E. Edmond.** 1979. Herpesviruses. J. Clin. Pathol. 32: 859–881.
23. **Torre, D., R. Mancuso, and P. Ferrante.** 2005. Pathogenic mechanisms of meningitis/encephalitis caused by human herpesvirus 6 in immunocompetent adult patients. Clin. Infect. Dis. 41:422–423.
24. **Traverso, M., M. Malnati, C. Minetti, S. Regis, S. Tedeschi, M. Pedemonte, C. Bruno, R. Biassoni, and F. Zara.** 2006. Multiplex real-time PCR for detection of deletions and duplications in dystrophin gene. Biochem. Biophyse Res. Commun. 339:145–150.
25. **Visser, A. M., G. J. J. van Doornum, J. J. Cornelissen, and M. J. van den Bent.** 2005. Severe amnesia due to HHV-6 encephalitis after allogenic stem cell transplantation. Eur. Neurol. 54:233–234.
26. **Wadowsky, R. M., S. Laus, M. Green, S. A. Webber, and D. Rowe.** 2003. Measurement of Epstein-Barr virus DNA loads in whole blood and plasma by TaqMan PCR and in peripheral blood lymphocytes by competitive PCR. J. Clin. Microbiol. 41:5245–5249.
27. **Yang, J., Q. Tao, L. W. Flinn, P. G. Murray, L. E. Post, H. Ma, S. Piantadosi, M. A. Caligiuri, and R. F. Ambinder.** 2000. Characterization of Epstein-Barr virus-infected B cells in patients with posttransplantation lymphoproliferative disease: disappearance after rituximab therapy does not predict clinical response. Blood 96:4055–4063.
28. **Yoshikawa, T.** 2004. Human herpesvirus 6 infection in hematopoietic stem cell transplant patients. Br. J. Haematol. 124:421–432.
29. **Zipeto, D., S. Morris, C. Hong, A. Dowling, R. Wolitz, T. C. Merigan, and L. Rasmussen.** 1995. Human cytomegalovirus (CMV) DNA in plasma reflects quantity of CMV DNA present in leukocytes. J. Clin. Microbiol. 33:2607–2611.

Psychiatry and Clinical Neurosciences (2007), **61**, 335 doi:10.1111/j.1440-1819.2007.01669.x

Letter to the Editor

Limbic encephalitis with autoantibodies against the glutamate receptor epsilon 2 mimicking temporal lobe epilepsy

The N-methyl-D-aspartate-type glutamate receptor epsilon 2 (GluR ε2) channels have been implicated in synaptic plasticity associated with neural development and learning. Recently, autoantibodies against GluR ε2 were found in some patients with Rasmussen's encephalitis[1] and non-herpetic limbic encephalitis.[2] This is a first case report of non-herpetic limbic encephalitis with autoantibodies against GluR ε2 showing neither MRI signal alterations nor abnormal cerebrospinal fluid (CSF) findings.

The patient was a 20-year-old woman with no prior history of neuropsychiatric disorders. She had insomnia, palpitations, anorexia, and general fatigue for 2 months prior to admission; these symptoms worsened gradually. Five days before admission, she developed rapidly recurring complex partial seizures (CPS) characterized by a motionless stare and unresponsiveness. EEG revealed ictal discharges beginning from the left temporal area.

Her body temperature was 37.9°C. Neurological examination was normal except for potentiation of her deep tendon reflexes in four limbs. Peripheral blood leukocyte count was 9400/μL. Biochemical blood studies were normal. Routine CSF studies showed no abnormalities; protein was 23 mg/dL and cell count was 2/μL. Polymerase chain reaction did not detect herpes simplex virus-1 or -2, human herpes virus-6 or -7, cytomegalovirus, or Epstein-Barr virus in CSF. MRI at 1.5 tesla did not reveal any signal alterations in her brain. CPS was controlled by the intravenous administration of diazepam. Surprisingly, Tc-99m SPECT on day 12 showed hyperperfusion in the left temporal lobe although the epileptic seizures had already disappeared. She recovered completely around day 50 following diverse neuropsychiatric symptoms such as transient aphasia, visual hallucinations, and emotional instability. SPECT showed disappearance of hyperperfusion in the left temporal lobe. Later, IgG autoantibodies against GluR ε2 were detected in CSF. During a follow-up period of 2 years, she has not developed any epileptic seizures. IgG autoantibodies against GluR ε2 disappeared in collection of CSF 2 years after her discharge.

We initially diagnosed her as having temporal lobe epilepsy since neither MRI nor CSF studies suggested encephalitis. However, SPECT showed hyperperfusion in her left temporal lobe although she was free from epileptic seizures. Moreover, she suffered from diverse neuropsychiatric symptoms following CPS for 50 days that could not be explained solely by postictal confusion. However, a limbic encephalitis could not be diagnosed definitely because no clear evidence of encephalitis was obtained until autoantibodies against GluR ε2 were detected.

Although the patient's encephalitis may have been caused by an undetected infectious agent, we propose a different explanation. A cell-mediated immune response may have caused tissue damage during an infectious episode before admission, resulting in the production of autoantibodies against GluR ε2. Alternatively, antibodies developing in response to an infectious agent may later have acted as autoantibodies against GluR ε2 because of molecular homology.

REFERENCES

1. Takahashi Y, Mori H, Mishina M *et al.* Autoantibodies to NMDA receptor in patients with chronic forms of epilepsia partialis continua. *Neurology* 2003; **61**: 891–896.
2. Mochizuki Y, Mizutani T, Isozaki E, Ohtake T, Takahashi Y. Acute limbic encephalitis: a new entity? *Neurosci. Lett.* 2006; **394**: 5–8.

AIHIDE YOSHINO, MD[1]
YOSHIE KIMURA, MD[1]
MASAKI MIYAZAKI, MD[1]
TETSUO OGAWA, MD[1]
AKI MATSUMOTO, MD[1]
SOICHIRO NOMURA, MD[1]
HIDEAKI NEMOTO, MD[2]
YUKITOSHI TAKAHASHI, MD[3]

[1]Department of Psychiatry, National Defense Medical College, Saitama, [2]Department of Neurology, Kohnodai Hospital, National Center of Neurology and Psychiatry, Chiba, and [3]Department of Pediatrics, National Epilepsy Center, Shizuoka Institute of Epilepsy and Neurological Disorders, Shizuoka, Japan

Correspondence address: Aihide Yoshino, MD, Department of Psychiatry, National Defense Medical College, 3-2 Namiki, Tokorozawa, Saitama 359-8513, Japan. Email: aihide@ndmc.ac.jp

Received 28 December 2006; accepted 11 February 2007.

INTERNAL MEDICINE

□ CASE REPORT □

Virus Associated Hemophagocytic Syndrome Accompanied by Acute Respiratory Failure Caused by Influenza A (H3N2)

Masaru Ando[1], Eishi Miyazaki[1], Shigeo Hiroshige[1], Yoshinori Ashihara[1], Toshiyuki Okubo[1], Mami Ueo[1], Tetsujiro Fukami[1], Katsunori Sugisaki[1], Tomiyasu Tsuda[4], Kazunari Ohishi[3], Shigenori Yoshitake[3], Takayuki Noguchi[3] and Toshihide Kumamoto[2]

Abstract

A 40-year-old Japanese woman was admitted to Oita University Hospital with progressive dyspnea, consciousness disturbance and severe cytopenias. Her chest roentgenogram showed diffuse bilateral infiltrates. She was therefore forced to receive mechanical ventilation. Bone marrow aspiration disclosed numerous hemophagocytic histiocytes, thus suggesting her condition to be hemophagocytic syndrome. In addition, she also developed myocarditis and renal failure. Pulsed methylprednisolone, gamma-globulin, granulocyte colony-stimulating factor and sivelestat sodium hydrate were administrated, and thereafter the patient recovered from cytopenia and organ failure. Afterwards, influenza A H3N2 was detected from bronchial extracts. We should recognize that an influenza A virus infection can induce hemophagocytic syndrome and acute respiratory failure as the initial manifestations of multiple organ failure.

Key words: virus-associated hemophagocytic syndrome, acute respiratory failure, influenza

(DOI: 10.2169/internalmedicine.45.1736)

Introduction

Influenza is defined as an acute respiratory illness that includes the upper and/or lower respiratory tracts and it is characterized by the abrupt onset of systemic signs and symptoms such as fever, headache, myalgia, arthralgia, malaise and weakness. Although an Influenza H3N2 infection shows a relatively favorable outcome, critical organ failure may rarely occur in compromised hosts, such as elderly people and patients with either diabetes mellitus or malignancies (1).

Hemophagocytic syndrome (HPS) is a clinicopathological entity characterized by peripheral blood cytopenias with marked hemophagocytosis in the bone marrow (2, 3). Patients with HPS often undergo an aggressive clinical course resulting in a poor prognosis. Virus-associated hemophagocytic syndrome (VAHS) occurs in association with a viral infection (2, 3); however, VAHS induced by influenza A is extremely rare. We herein describe a 40-year-old woman with VAHS accompanied by severe respiratory failure, myocarditis and acute renal failure associated with an Influenza H3N2 infection who was successfully treated by intensive medical care.

Case Report

A 40-year-old woman was admitted to Oita University Hospital because of progressive dyspnea and a consciousness disturbance. She had undergone a surgical resection for lingual carcinoma 2 years previously. After adjuvant chemotherapy and radiotherapy, she had since demonstrated a

[1] Division of Pulmonary Disease, Oita University Faculty of Medicine, Oita, [2] Division of Neurology and Neuromuscular Disorders, Oita University Faculty of Medicine, Oita, [3] Division of Diseases and Therapy, Department of Brain and Nerve Science, Oita University Faculty of Medicine, Oita and [4] Shin-Beppu Hospital, Beppu

Received for publication January 23, 2006; Accepted for publication July 3, 2006

Correspondence to Dr. Masaru Ando, Division of Pulmonary Disease, Department of Brain and Nerve Science, Oita University Faculty of Medicine, 1-1 Idaigaoka, Hasama-machi, Oita 879-5593

DOI: 10.2169/internalmedicine.45.1736

Table 1. **Serological Data on Admission and on the 14th Hospital Day**

		2002/12/31	2003/1/13
Influenza type A Moscow/13/98(H1N1)		x80	x80
Influenza type A New Caledonia/20/99(H1N1)		x80	x80
Influenza type A Panama/2007/99(H3N2)		x40	x640
Influenza type B Hiroshima/23/01		x20	x20
Legionella Ab		<64	<64
Cytomegalovirus	IgG	95.0	57.5
	IgM	0.26	0.46
Chlamydia pneumonia	IgG	1.23	1.82
	IgA	1.02	1.94

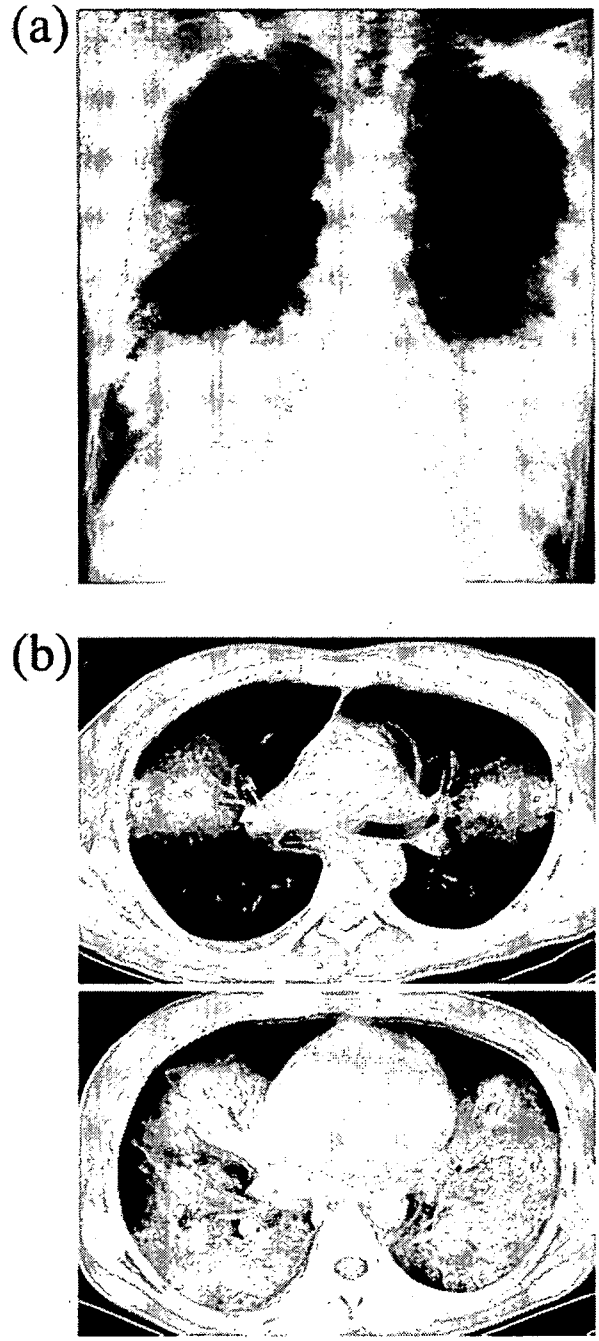

Figure 1. **Chest images on admission: (a) chest roentgenogram demonstrates bilateral infiltrates predominantly on the middle and lower lung fields; (b) chest CT scan demonstrates bilateral air-space consolidation, diffuse ground-grass attenuation and a small amount of pleural effusion.**

complete remission of the disease. On December 28, 2002, she developed high fever, chills and non-productive cough and thus visited the nearby hospital on December 30. Her chest roentgenogram showed bilateral infiltrates. A rapid detection test for influenza virus antigen showed a negative result and therapy with imipenem cilastatin sodium, and clindamycin in addition to γ-globulin was thus started. The next day, her leukocyte and platelet counts suddenly decreased from 3,800 /μl to 400/ μl, and from 14.6×10^4/ μl to 4.7×10^4/ μl, respectively, and therefore she was immediately transferred to our hospital. On admission, her blood pressure was 66/49 mmHg, pulse rate 130/min, respiratory rate 37/min, and temperature 37 degree. Coarse crackles were audible bilaterally at the base of her lung. The leukocyte count was 200/ μl, the erythrocyte count 407×10^4/ μl, and the platelet count 2.3×10^4/ μl, respectively. The hemoglobin level was 9.8 g/dl. Other laboratory values were as follows: C-reactive protein (CRP) 41.03 mg/dl, total protein 5.33 g/dl, albumin 3.19 g/dl, creatinine kinase (CK) 862 IU/l, aspartate aminotransferase (GOT) 61.4 IU/l, alanine aminotransferase (GPT) 17.1 IU/l, lactate dehydrogenase (LDH) 805 IU/l, blood urea nitrogen (BUN) 46.71 mg/dl, creatinine (Cr) 3.53 mg/dl, fibronogen 444 mg/dl. Antinuclear antibodies were negative. Soluble interleukin-2 receptor was elevated with a value of 3,780 U/l. A blood gas analysis showed hypocarbonic hypoxemia with PaO_2 of 59.1 Torr and $PaCO_2$ of 33.3 Torr in providing 10 L/min oxygen with facial mask (Table 1). On chest X-ray, diffuse bilateral infiltrates were found (Fig. 1a) and chest computed tomography scans demonstrated airspace consolidation on the bilateral lower lung fields, diffuse ground glass attenuation predominantly in the middle lung fields and a small amount of pleural effusion (Fig. 1b). Bone marrow aspiration was done on the day of admission, thus demonstrating hypocellular marrow with 4% hemophagocytic histiocytes in which red blood cells, platelets, or neutrophils were captured (Fig. 2). Due to her clinical manifestation of HPS, acute respiratory failure was suggested to be due to some infections or drugs. Repeated measurements of influenza virus antigen in serum and bron-

DOI: 10.2169/internalmedicine.45.1736

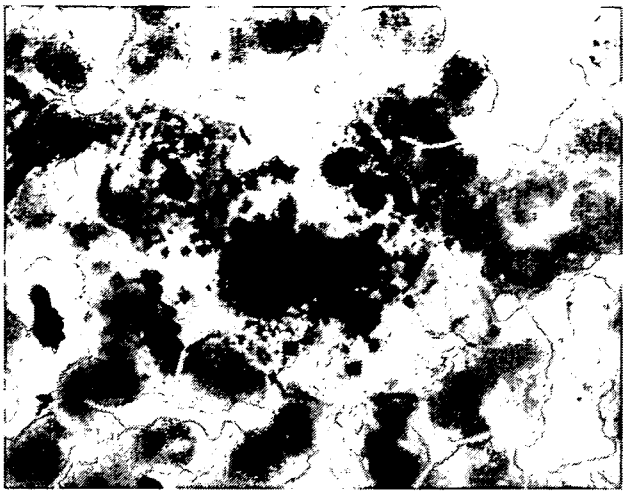

Figure 2. **A bone marrow smear shows histiocytic cells phagocytosing neutrophils, erythroblasts and platelets (May-Giemsa stain, ×1,000, original magnification).**

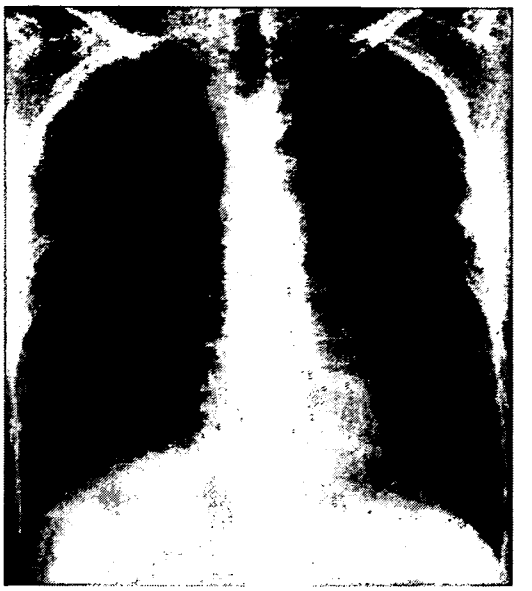

Figure 3. **A chest roentgenogram shows an extreme reduction of bilateral infiltrates on the 12th hospital day.**

chial extract were negative. Drug lymphocyte stimulation tests for imipenem cilastatin sodium and clindamycin were negative.

No infectious bacterial pathogens could be isolated from either blood and bronchial extracts. Bronchoalveolar lavage (BAL) could not be performed because the patient had severe hypotension (66/49 mmHg) and hypoxemia (P/F ratio: 58.6). The patient required mechanical ventilation and was treated with pulsed methylprednisolone (mPSL, 1,000 mg/day for 3 days), γ-globurin (5 g/day for 3 days), and 500 μg of granulocyte colony-stimulating factor (G-CSF). Concurrently, sivelestat sodium hydrate, which is a neutrophil elastase inhibitor (200 mg/day for 11 days), tetracycline (100 mg/day for 9 days) and ciprofloxacin (300 mg/day for 6 days) were administered. At twelve hours after admission, an electrocardiogram revealed an elevated T wave at every channel other than aVR with some ventricular premature contraction (VPC). An echocardiogram showed diffuse impaired myocardial movement without asymmetry. She was diagnosed to have myocarditis, and thus was treated with nitroglycerine and nicorandil. The CK level in the serum reached a peak (11,942 IU/l) on the third hospital day and then gradually subsided.

The leukocyte count on the forth hospital day increased to 9,400/ μl and bone marrow smear on the sixth hospital day showed the disappearance of hemophagocytic histiocytes. Since the BUN and Cr levels were high, while the urine volume had decreased, continuous hemodiafiltration (CHDF) was started on the forth hospital day. After CHDF was performed for four days, her renal function recovered. After such intensive therapies, the patient's respiratory insufficiency gradually improved and her chest X-ray became clear (Fig. 3). She was extubated on the 12th hospital day. Finally, the patient's organ failure completely recovered without any lingering symptoms.

We measured the antibody titers of several pathogens in the stocked sera on the first and the 14th hospital day. We obtained serological evidence of a previous infection with adeno, parainfluenza, cytomegalo and Ebstain-Barr viruses. No antibodies to influenza B and respiratory syncytial viruses were found. The antibody to Influenza A Panama virus (H3N2) had increased from ×40 to ×640 (Table 1). In addition, the Influenza H3N2 virus was isolated from a bronchial extract specimen obtained on the second hospital day.

Discussion

The present patient developed VAHS, acute respiratory failure, myocarditis and acute renal failure due to the Influenza A H3N2 virus, which was isolated from a respiratory specimen. She was treated with pulsed m-PSL and γ-globulin, G-CSF and sivelestat sodium hydrate and thereafter recovered completely.

VAHS was first described by Risdall et al in 1979 in a series of 19 patients with peripheral blood cytopenias associated with marrow hemophagocytosis (2). It occurs most commonly in association with the herpes group viruses, in particular cytomegalovirus and the Epstein-Barr virus (2-4). Influenza A virus-associated HPS is extremely rare, and has been reported in a cluster of three children who received chemotherapy for acute leukemia (5). Two cases spontaneously recovered, while the remaining one died of cardiorespiratory failure secondary to *Klebseilla pneumonia* septicemia. Two sporadic cases with influenza A associated HPS with pernicious anemia and alcoholism as underlying diseases were also reported (3, 6); however, these abovementioned reports did not elucidate the subtypes of the Influenza A virus. In a recent outbreak of an avian Influenza A H5N1 infection in Hong Kong in 1997, six of eighteen patients died as a result of ARDS or MOF, and two among

DOI: 10.2169/internalmedicine.45.1736

these six fatal cases showed reactive HPS as the most prominent feature (7). Our patient is the first confirmed case of an Influenza A H3N2 infection who developed VAHS accompanied by MOF including acute respiratory failure, myocarditis and acute renal failure and who subsequently survived owing to appropriate intensive care.

We do not have any precise explanation why this patient developed MOF after an infection with Influenza H3N2, the most common subtype of influenza. While underlying cardiovascular, pulmonary and renal diseases, alcoholism and pregnancy have been regarded as the major predisposing factors for a severe influenza A infection (8), none of these factors were found in our patient. It is unlikely that she has a systemic immunosuppressive condition, but structural alterations after neck surgery may have affected her local immunological system.

The pathogenesis of VAHS is still obscure; however, a cytokine-driven condition triggered by a viral replication is postulated (7). In this context, immunosuppressive therapy, especially high-dose corticosteroid may contribute to cytokine regulation. As this patient did not undergo antiviral treatment, the immediate administration of pulsed m-PSL appeared to improve the symptoms of cytopenia and subsequent organ failure by regulating hypercytokinemia. In addition, high-dose γ-globulin and G-CSF therapy has been reported to be effective for the treatment of HPS, thus resulting in a favorable prognosis (9, 10).

We should recognize that an Influenza virus A H3N2 infection may induce VAHS, acute respiratory failure and eventually MOF in apparently healthy middle-aged individuals. These complications caused by the Influenza H3N2 infection were found to be reversible by the administration of aggressive immunosuppressive therapies including pulsed m-PSL, γ-globulin, G-CSF and sivelestat sodium hydrate.

We thank Dr. T. Imamura and Dr. E. Ohtsuka, Department of Infectious Diseases and Prevention, Oita University Faculty of Medicine for valuable help with the bone marrow analysis, and Mr. T. Ono, Mr. S. Yoshiyo and Mr. M. Ogawa , Oita Prefectural Institute of Health and Environment for assistance with the serological analysis for influenza viruses and the detection of the influenza A virus.

References

1. Dolin R. Influenza. in: Harrison's Principles of Internal Medicine. 14th ed. Isselbacher KJ, Braunwald E, Wilson JD, et al, Eds. McGraw-Hill, New York, 1994: 814-819.
2. Risdall RJ, McKenna RW, Nesbit ME, et al. Virus-associated hemophagocytic syndrome: a benign histiocytic proliferation distinct from malignant histiocytosis. Cancer **44**: 993-1002, 1979.
3. Reiner AP, Spivak JL. Hematophagic histiocytosis. A report of 23 new patients and a review of the literature. Medicine (Baltimore) **67**: 369-388, 1988.
4. Reisman RP, Greco A. Virus-associatd hemophagocytic syndrome due to Epstein-Barr virus. Hum Pathol **15**: 290-293, 1984.
5. Potter MN, Foot AB, Oakhill A. Influenza A and the virus associated haemophagocytic syndrome: cluster of three cases in children with acute leukaemia. J Clin Pathol **44**: 297-299, 1991.
6. Shirono K, Tsuda H, Akahoshi I. Influenza-virus associated hemophagocytic syndrome in a patient with pernicious anemia. Rinsho Ketsueki **37**: 511-513, 1996 (in Japanese).
7. To KF, Chan PK, Chan KF, et al. Pathology of fatal human infection associated with avian influenza A H5N1 virus. J Med Virol **63**: 242-246, 2001.
8. Kilbourne ED. Epidemiology of influenza. in: The Influenza Viruses and Influenza. Kilbourne ED, Ed. Academic Press, London, 1995: 483-538.
9. Tsuda H, Shirono K. Successful treatment of virus-associated haemophagocytic syndrome in adults by cyclosporin A supported by granulocyte colony-stimulating factor. Br J Haematol **93**: 572-575, 1996.
10. Oyama Y, Amano T, Hirakawa S, Hironaka K, Suzuki S, Ota Z. Haemophagocytic syndrome treated with cyclosporin A: a T cell disorder? Br J Haematol **73**: 276-278, 1989.

Functional Neuroscience: Evoked Potentials and Related Techniques
(Supplements to Clinical Neurophysiology, Vol. 59)
Editors: C. Barber, S. Tsuji, S. Tobimatsu, T. Uozumi, N. Akamatsu, A. Eisen

Chapter 36

Immune-mediated potassium channelopathies

Kimiyoshi Arimura*, Arlene R. Ng and Osamu Watanabe

Department of Neurology and Geriatrics, Kagoshima University Graduate School of Medical and Dental Sciences, Kagoshima, 890-8520 (Japan)

1. Introduction

Ion channelopathies are largely classified as either hereditary or acquired. Hereditary channelopathies are due to mutations of ion channel genes, which produce abnormal channel proteins that either fail to function or function in an abnormal manner. On the other hand, acquired channelopathies are either due to the targeting of channels by autoantibodies (immune-mediated channelopathies), drugs and toxins, or the dysregulated expression of an inappropriate repertoire of ion channels in the absence of abnormal channel structures.

The concept of immune-mediated channelopathies was first recognized in neuromuscular junction disorders where the acetylcholine receptor was found to be the target channel protein in myasthenia gravis and the voltage-gated calcium channel was involved in Lambert–Eaton myasthenic syndrome. Recently, rapid progress in the fields of genetics, immunology, and molecular biology have led to the discovery of new ion channel disorders in the peripheral and central nervous system (CNS). One such group of disorders affect voltage-gated potassium channels (VGKCs).

Correspondence to: Kimiyoshi Arimura, M.D., Ph.D., Department of Neurology and Geriatrics, Kagoshima University Graduate School of Medical and Dental Sciences, 8-35-1 Sakuragaoka, Kagoshima, 890-8520, Japan.
Tel: +81-99-275-5332; Fax: +81-99-265-7164;
E-mail: ari@m2.kufm.kagoshima-u.ac.jp

VGKCs have a multimeric structure composed of 4 α-subunits produced by separate genes (heteromultimeric). Each α-subunit has 6 transmembrane components. In the axons, VGKCs are activated by depolarization. They regulate the resting membrane potential and control the shape and frequency of action potentials. After depolarization, VGKCs are important in repolarizing the axon membrane. If K^+ channel function is suppressed, the depolarization of the axon membrane will be prolonged and induce repetitive firing of action potentials. Two types of K^+ channels have been identified, fast and slow. Fast K^+ channels are located at the paranodal regions and are normally masked by myelin, while slow K^+ channels and inward rectifiers are mainly located at the internodal regions.

At present, several K^+ channelopathies in the nervous system, both hereditary and acquired, have already been identified. Included under the hereditary K^+ channelopathies are episodic ataxia/myokymia syndrome, myokymia and benign neonatal epilepsy, and benign neonatal epilepsy. Paroxysmal choreoathetosis/spasticity is also suspected to be linked to K^+ channel dysfunction. Under the immune-mediated K^+ channelopathies involving the peripheral nervous system are acquired neuromyotonia (Isaacs' syndrome) and cramp-fasciculation syndrome, while those involving the CNS include Morvan's fibrillary chorea and limbic encephalitis. This chapter will center on

immune-mediated K^+ channelopathies in the central and peripheral nervous systems.

2. Isaacs' syndrome

Isaacs' syndrome, or acquired neuromyotonia, is characterized by generalized muscle stiffness, cramps, myokymia, and delayed relaxation. Electromyographic findings show myokymic and neuromyotonic discharges as well as continuous motor unit activity that are related to spontaneous repetitive firing of motor nerves. Myokymic discharges are repetitive discharges firing at rates of 5–150 Hz and may appear as doublets, triplets, or multiplets. Neuromyotonic discharges, on the other hand, fire at rates of 150–300 Hz. They often begin and end abruptly, persist only up to a few seconds and the amplitudes of the discharges typically wane (Gutmann and Gutmann, 2004).

2.1. Pathophysiology of Isaacs' syndrome

Three main points can be gleaned from studies relating to the possible pathophysiologic mechanism behind Isaacs' syndrome. First is that, based on electrophysiologic and pharmacologic studies, the peripheral motor nerves are hyperexcitable. Using a method developed by Bostock et al. (1998), Madison et al. (1999) reported the results of direct measurements of nerve hyperexcitability in Isaacs' patients. They found that, compared to healthy controls, a shorter stimulus duration was required to produce the threshold current. This implies increased excitability of the nodal membrane which, in turn, could be caused by an ectopic focus. This is also supported by findings that anti-epileptic drugs and Na^+ channel antagonists reduce symptoms and signs. Second, VGKCs may be involved, as suggested by passive transfer studies in mice (Sinha et al., 1991). Lastly, anti-VGKC antibodies may be causative in Isaacs' syndrome. Our own studies using western blotting have shown the presence of anti-VGKC antibodies in a patient's serum. The patient's γ-globulin bound to 50 kDa proteins of PC-12 cell lysates which, in turn, cross-linked with α-dendrotoxin, a novel toxin that binds VGKCs (Fig. 1A). Immunohistochemical staining also showed that the patient's serum reacted to PC-12 cell membranes and growth cones, where there is an increased number of VGKCs (Fig. 1B; Arimura et al., 1997). Other immunologic studies have likewise confirmed the presence of anti-VGKC antibodies in patients with Isaacs' syndrome (Newsom-Davis and Mills, 1993; Shillito et al., 1995; Hart et al., 1997, 2002).

2.2. Detection of antibodies to VGKCs

The detection of anti-VGKC antibodies can be performed using several methods. In most occasions, immunoprecipitation with α-dendrotoxin, a toxin that binds specifically to VGKC, and patch-clamp methods are used. Immunoprecipitation is easy to perform and highly specific for detecting anti-VGKC antibodies; however, sensitivity may be lower compared to the patch-clamp method (unpublished data). On the other hand, the patch-clamp method, although time consuming, has a much higher sensitivity in detecting VGKC dysfunction. The reason for this higher sensitivity compared to immunoprecipitation is that the patch-clamp method can detect the presence not only of anti-VGKC antibodies but also antibodies against other molecules that affect VGKC function. Figure 2 shows the results of immunoprecipitation of patients' sera with α-dendrotoxin. In acquired neuromyotonia (ANM) patients, anti-VGKC IgG antibody was shown to be elevated in the serum. Control subjects and GBS patients, however, did not show the same elevation (unpublished data).

We performed the patch-clamp method in studying the pathomechanism of antibody involvement in VGKCs. K^+ currents of cultured cells (PC-12 or NB-1) were measured after incubation with either patients' sera or immunoglobulins from control subjects. As shown in Fig. 3A, outward K^+ currents of PC-12 cells were significantly suppressed by patients' sera after co-culturing for 6 days (Sonoda et al., 1996). The same results were obtained using the NB1 cultured cell line. Voltage-gated Na^+ channel was not significantly suppressed (Fig. 3B; Nagado et al., 1999).

The suppression of VGKCs by the patch-clamp method also correlated significantly with neuromyotonic and myokymic discharges. However, it had no significant correlation with clinical myokymia and fasciculations (unpublished data).

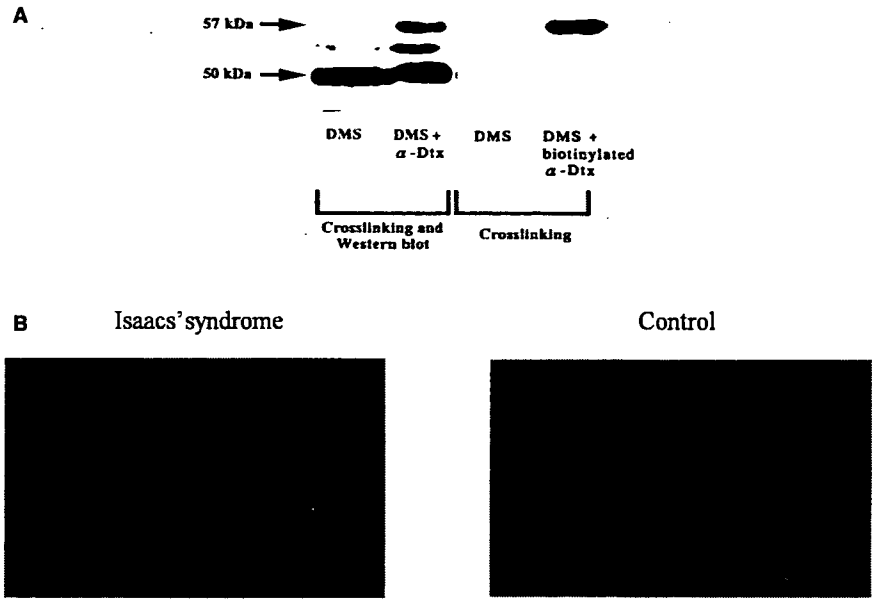

Fig. 1. (A) γ-Globulin of a patient with Isaacs' syndrome bound to a 50 kDa protein of PC-12 cell lysates. This same 50 kDa protein cross-linked with α-dendrotoxin, a toxin which binds VGKCs. (B) The same patient's serum reacted to PC-12 cell membranes and growth cones, a finding which was not documented in the control serum. (Taken from Arimura et al. (1997) Antibodies to potassium channels of PC12 in serum of Isaacs' syndrome: Western blot and immunohistochemical studies. *Muscle Nerve*, 20, Copyright © 1997 Wiley Periodicals, Inc.)

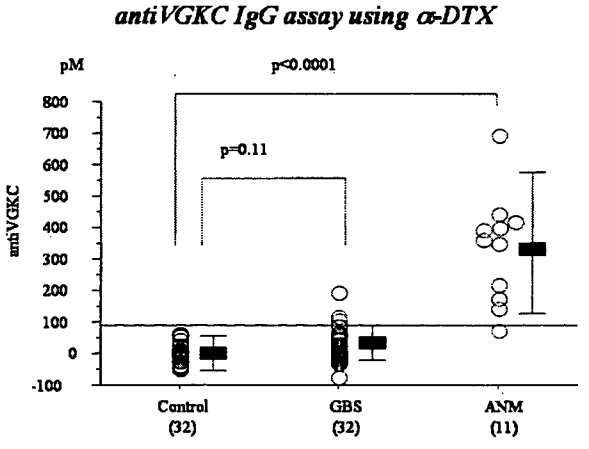

Fig. 2. Immunoprecipitation with α-dendrotoxin showed that sera of ANM patients had elevated anti-VGKC IgG antibody compared to GBS and control sera.

2.3. Pathomechanism of the suppression of VGKCs by anti-VGKC antibodies

Based on the knowledge gained from a considerable number of studies in myasthenia gravis, suppression of channel function may roughly be classified as follows:

(1) antibodies cross-link channel proteins and induce increase in channel degradation;
(2) antibodies bound to complements reduce channels;
(3) antibodies block channel pores where ions pass; and
(4) antibodies bind proteins which regulate channel kinetics.

Our patch-clamp studies have shown that suppression of VGKC by anti-VGKC antibodies was time dependent. Six days after co-culturing with a patient's serum, both the steady state and peak potassium currents of PC-12 cells were markedly suppressed compared to control. There was no significant change

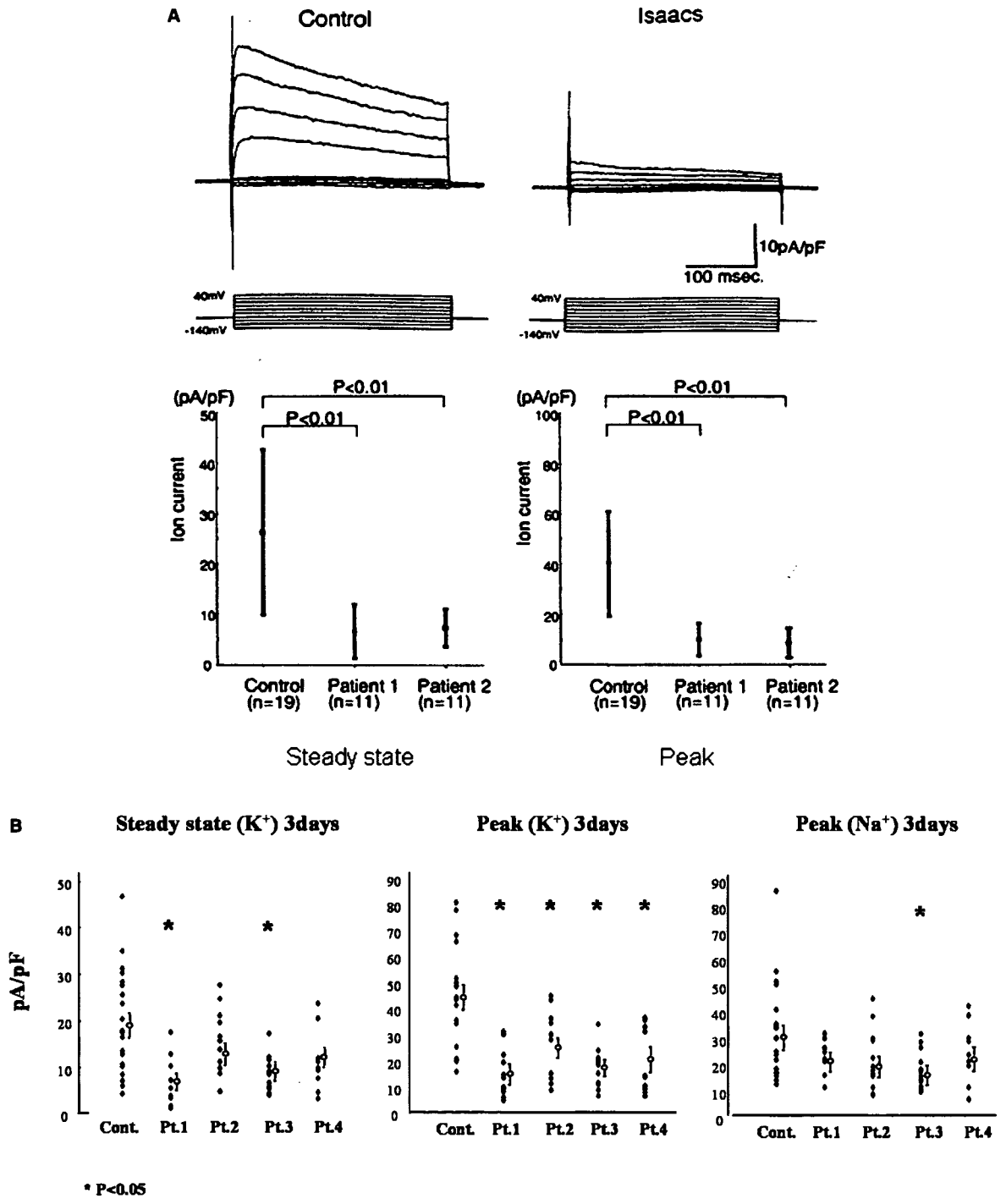

Fig. 3. (A) Outward potassium currents of PC-12 cells were significantly suppressed by patients' sera after co-culturing for 6 days. (Taken from Sonoda et al. (1996) Serum of Isaacs' syndrome suppresses potassium channels in PC-12 cell lines. *Muscle Nerve*, 19, Copyright © 1996 Wiley Periodicals, Inc.) (B) Similar results of outward K^+ current suppression were observed in NB1 cells after co-culturing with patients' sera for 3 days.

in the values of net ion currents before and immediately after direct addition of the patient's serum. These findings suggest that antibodies may not directly block channel kinetics but may decrease channel densities. To confirm this hypothesis, we studied the effects of antibodies on channel kinetics and found that voltage-dependent channel activation and inactivation did not differ significantly from those of controls. Single channel conductance was likewise not altered (Nagado et al., 1999).

In order to clarify how antibodies reduce K^+ currents in neuronal cell lines, we studied the effects of monovalent Fab and Fc, and divalent Fab fractions of immunoglobulins, obtained by addition of papain and pepsin respectively, using whole-cell clamp methods. The Fc and monovalent Fab fractions had no effect on K^+ currents, but divalent Fab fractions substantially reduced K^+ currents in a manner resembling whole IgG. This result indicates that cross-linking of VGKCs by divalent Fab fractions is important in altering channel function (Tomimitsu et al., 2004).

We also investigated the effect of complement on VGKC function by measuring K^+ currents after adding 40 u/ml guinea pig complement using the patch-clamp method. Complement addition did not increase the effect of the IgG in reducing VGKC current. This indicates that complement-mediated damage is not involved in the pathogenesis of Isaacs' syndrome (Tomimitsu et al., 2004). Taken together, these findings may point to an increase in the degradation rate of VGKCs by cross-linking of anti-VGKC antibody, especially divalent Fab, with channel proteins, a finding which has been reported in myasthenia gravis (Drachman et al., 1978).

2.4. Site of origin of repetitive discharges

The spontaneous activity in Isaacs' syndrome arises from peripheral nerves since it persists during general anesthesia and is abolished by curare-induced blockade of neuromuscular transmission. The main generator sites are suspected to be located at the distal portion of the motor nerve, within the terminal arborization, which lies outside the blood nerve barrier (Newsom-Davis and Mills, 1993; Arimura et al., 1997; Vincent, 2000). However, variable persistence of spontaneous activity after proximal nerve block has also led to the assumption that generator sites may also exist more proximally, may be even at the level of the anterior horn cell (Newsom-Davis and Mills, 1993).

To further clarify the exact sites of origin of repetitive discharges, we performed macro EMG and quantitative EMG studies during voluntary contraction and at rest. Motor unit potential size analysis by macro EMG triggered by single muscle fiber action potentials allows the estimation of an approximate number of muscle fibers which belong to the same motor unit (Stålberg, 1983). By comparing the macro MUP triggered by spontaneous discharges to that triggered by voluntary contraction, it is possible to speculate the site of origin of spontaneous discharges electrophysiologically. If the origin was located distal to the nerve branching, the macro MUP triggered by spontaneous discharges may be smaller than those triggered by voluntary contraction. Results of macro EMG clearly show that both amplitude and area of macro MUP triggered by myokymic discharges are significantly smaller than those triggered by voluntary contraction. These indicate that the sites of origin of spontaneous discharges may be located at the most distal part of the motor nerve, mainly after the terminal arborization and at the nerve terminals. In fact, Oda et al. (1989) reported that terminal sprouting is frequently seen in ANM. These terminals may be hyperexcitable because of the accumulation of Na^+ channels. We also performed immunohistochemical staining of a biopsied muscle specimen from a normal subject with serum from patient 2. Positive staining of axons of an intramuscular nerve further supports involvement of VGKCs at the most distal part of the nerve (Arimura et al., 1997).

2.5. Location of ion channels

The process of saltatory conduction is highly dependent on ion channel location and compartmentalization at the nodes of Ranvier of myelinated axons. Indeed, mammalian peripheral axons have few VGKCs at

the node rendering them less accessible to anti-VGKC antibodies. VGKCs located in somatodendritic regions play important roles in regulating neuronal firing (Dodson and Forsythe, 2004). Fast K^+ channels, which are mainly involved in neuromyotonia, are prevalent in the axonal and final segment of the axon. In the final segment of peripheral nerves, these channels are localized in the transition zone between the myelinated portion and synaptic terminal. They are absent at the synaptic terminal itself (Chiu et al., 1999). It is also known that the blood nerve barrier is absent not only in the synaptic terminal but also in this transition zone. On the other hand, fast K^+ channels of the nerve trunk are located at the juxtaparanode where they are covered by myelin sheath and the blood–nerve barrier is known to exist (Chiu and Ritchie, 1980). Based on the above results of macro EMG studies and the known localization of VGKCs, we can conclude that the origin of spontaneous discharges in Isaacs' syndrome is located at the most distal part of the axon, including the transition zone.

3. Immune-mediated potassium channelopathies in the CNS

Immune-mediated potassium channelopathies with positive anti-VGKC antibodies are also found in disorders of the CNS. The correlation between anti-VGKC antibodies and CNS disorders was first described in Morvan's fibrillary chorea (Liguori et al., 2001). Subsequently, anti-VGKC antibodies were also found in 2 patients with limbic encephalitis (Buckley et al., 2001).

Morvan's syndrome shows characteristic manifestations of hyperexcitability in both central and peripheral nervous systems, namely neuromyotonia, dysautonomia, hyperhidrosis, anorexia, encephalopathy, severe insomnia, visual hallucination, and pruritus with atopic dermatitis. Limbic encephalitis, on the other hand, is typically a paraneoplastic syndrome with a poor prognosis. Vincent et al. (2004) recently reviewed the clinical, immunological, and neuropsychological features of 10 patients with this disorder. All patients presented with histories of memory loss, confusion, and seizures. Eight of 10 patients showed low plasma sodium concentrations; however, in contrast to Morvan's syndrome, neuromyotonia was rare. Brain MRI showed signal changes in the medial temporal lobes. Anti-VGKC antibodies were elevated in all patients. Variable treatment regimens of steroids, plasma exchange, and intravenous immunoglobulin produced marked improvement in psychological function in 6 patients associated with variable fall in serum anti-VGKC antibody levels. Based on these findings, it is advisable that patients who present with limbic encephalitis of unknown etiology undergo measurement of anti-VGKC antibody levels.

Anti-VGKC antibodies may also be correlated with the existence of intractable epilepsy of unknown

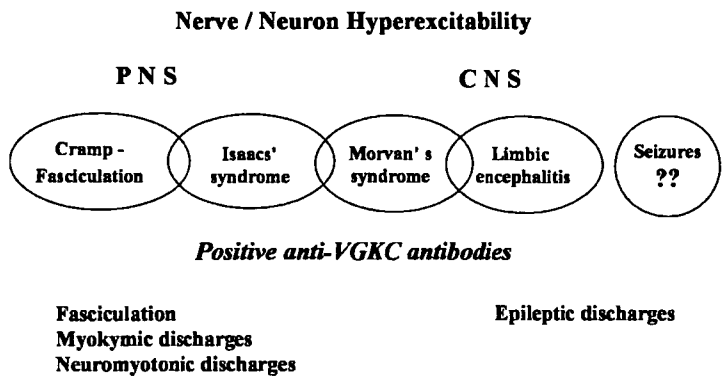

Fig. 4. Summary of immune-mediated potassium channelopathies in neurological disorders.

etiology. The pathomechanism of seizures, a manifestation of hyperexcitability in the CNS, is due to the suppression of VGKCs. The synchronous firing of neurons during a seizure may be due to the wiring together of these neurons through a process called axonal sprouting. The sprouted axons also provide additional positive feedback to the neurons in the epileptic network, facilitating further seizures. The loss of an inhibitory K^+ current, called the A current, which flows through A-type K^+ channels, may also contribute to this positive feedback and facilitates further epileptic seizures wirelessly, that is in the absence of axonal sprouting (Staley, 2004). In seizures of limbic encephalitis, such a wireless mechanism may occur due to the suppression of VGKC by anti-VGKC antibodies.

4. Conclusions

Figure 4 summarizes the relationship of immune-mediated potassium channelopathies in both the central and peripheral nervous systems, where antibodies against VGKCs are clearly correlated with nerve hyperexcitability. The concept of immune-mediated potassium channelopathies in the neurological field is now expanding. It is possible that with further progress in molecular biology, other diseases may also be classified as K^+ channelopathies in the near future. It is therefore important to have a high level of suspicion regarding the existence of anti-VGKC antibodies when a patient shows acquired signs and symptoms of nerve hyperexcitability of unknown origin.

References

Arimura, K., Watanabe, O., Kitajima, I., Suehara, M., Minato, S., Sonoda, Y., Higuchi, I., Takenaga, S., Maruyama, I. and Osame, M. (1997) Antibodies to potassium channels of PC12 in serum of Isaacs' syndrome: Western blot and immunohistochemical studies. *Muscle Nerve*, 20: 299–305.

Bostock, H., Cikurel, K. and Burke, D. (1998) Threshold tracking techniques in the study of human peripheral nerve. *Muscle Nerve*, 21: 137–158.

Buckley, C., Oger, J., Clover, L., Tuzun, E., Carpenter, K., Jackson, M. and Vincent, A. (2001) Potassium channel antibodies in two patients with reversible limbic encephalitis. *Ann. Neurol.*, 50: 73–78.

Chiu, S.Y. and Ritchie, J.M. (1980) Potassium channels in nodal and internodal axonal membrane of mammalian myelinated fibres. *Nature*, 284: 170–171.

Chiu, S.Y., Zhou, L., Zhang, C. and Messing, A. (1999) Analysis of potassium channel functions in mammalian axons by gene knockouts. *J. Neurocytol.*, 28: 349–364.

Dodson, P.D. and Forsythe, I.D. (2004) Presynaptic K^+ channels: electrifying regulators of synaptic terminal excitability. *Trends Neurosci.*, 27: 210–217.

Drachman, D.B., Angus, C.W., Adams, R.N., Michelson, J.D. and Hoffman, G.J. (1978) Myasthenic antibodies cross-link acetylcholine receptors to accelerate degradation. *New Engl. J. Med.*, 298: 1116–1122.

Gutmann, L. and Gutmann, L. (2004) Myokymia and neuromyotonia 2004. *J. Neurol.*, 251: 138–142.

Hart, I.K., Waters, C., Vincent, A., Newland, C., Beeson, D., Pongs, O., Morris, O. and Newsom-Davis, J. (1997) Autoantibodies detected to expressed K^+ channels are implicated in neuromyotonia. *Ann. Neurol.*, 41: 238–246.

Hart, I.K., Maddison, P., Newsom-Davis, J., Vincent, A. and Mills, K.R. (2002) Phenotypic variants of autoimmune peripheral nerve hyperexcitability. *Brain*, 125: 1887–1895.

Liguori, R., Vincent, A., Clover L., Avoni, P., Plazzi, G., Cortelli, P., Baruzzi, A., Carey, T., Gambetti, P., Lugaresi, E. and Montagna, P. (2001) Morvan's syndrome: peripheral and central nervous system and cardiac involvement with antibodies to voltage-gated potassium channels. *Brain*, 124: 2417–2426.

Maddison, P., Newsom-Davis, N. and Mills, K.R. (1999) Strength-duration properties of peripheral nerve in acquired neuromyotonia. *Muscle Nerve*, 22: 823–830.

Nagado, T., Arimura, K., Sonoda, Y., Kurono, A., Horikiri, Y., Kameyama, A., Kameyama, M., Pongs, O. and Osame, M. (1999) Potassium current suppression in patients with peripheral nerve hyperexcitability. *Brain*, 122: 2057–2066.

Newsom-Davis, J. and Mills, K.R. (1993) Immunological associations of acquired neuromyotonia (Isaacs' syndrome). *Brain*, 116: 453–469.

Oda, K., Fukushima, N., Shibasaki, H. and Ohnishi, A. (1989) Hypoxia-sensitive hyperexcitability of the intramuscular nerve axon in Isaacs' syndrome. *Ann. Neurol.*, 25: 140–145.

Shillito, P., Molenaar, P.C., Vincent, A., Leys, K., Zheng, W., Van den Berg, R.J., Plomp, J.J., Van Kempen, G. Th. H., Chauplannaz, G., Wintzen, A.R., Van Dijk, J.G. and Newsom-Davis, J. (1995) Acquired neuromyotonia: evidence for autoantibodies directed against K^+ channels of peripheral nerves. *Ann. Neurol.*, 38: 714–722.

Sinha, S., Newsom-Davis, J., Mills, K., Byrne, N., Lang, B. and Vincent, A. (1991) Autoimmune aetiology for acquired neuromyotonia (Isaacs' syndrome). *Lancet*, 338: 75–77.

Sonoda, Y., Arimura, K., Kurono, A., Suehara, M., Kameyama, M., Minato, S., Hayashi, A. and Osame, M. (1996) Serum of Isaacs' syndrome suppresses potassium channels in PC-12 cell lines. *Muscle Nerve*, 19: 1439–1446.

Stålberg, E. (1983) Macro EMG. *Muscle Nerve*, 6: 619–630.

Staley, K. (2004) Epileptic neurons go wireless. *Science*, 305: 482–483.

Tomimitsu, H., Arimura, K., Nagado, T., Watanabe, O., Otsuka, R., Kurono, A., Sonoda, Y. and Osame, M. (2004) Mechanism of action of voltage-gated K^+ channel antibodies in acquired neuromyotonia. *Ann. Neurol.*, 56: 440–444.

Vincent, A. (2000) Understanding neuromyotonia. *Muscle Nerve*, 23: 655–657.

Vincent, A., Buckley, C., Schott, J.M., Baker, I., Dewar, B.K., Detert, N., Clover, L., Parkinson, A., Bien, C.G., Omer, S., Lang, B., Rossor, M.N. and Palace, J. (2004) Potassium channel antibody-associated encephalopathy: a potentially immunotherapy-responsive form of limbic encephalitis. *Brain*, 127: 701–712.